AB INITIO MOLECULAR DYNAMICS SIMULATIONS OF MULTIMOLECULAR COLLISIONS OF NITROMETHANE AND COMPRESSED LIQUID NITROMETHANE

Stephen A. Decker and Tom K. Woo[*]
Department of Chemistry, University of Western Ontario,
London, ON, N6A 5B7, Canada

Dongqing Wei
Centre de Reserche en Calcule, Montreal, QB, H3X 2H9, Canada

Fan Zhang
Defence R&D Canada – Suffield, Medicine Hat, AB, T1A 8K6 Canada

[*] Author to whom correspondence should be addressed: e-mail: twoo@uwo.ca.

Our current interest focuses on the atomic level details of the decomposition mechanism of liquid NM under shock and highly compressed conditions, using Car-Parrinello *ab initio* molecular dynamics (CPMD) simulations. Multimolecular collision simulations indicate that neighboring molecules act as a trap to confine the recoiling fragments produced during the initial collision, thereby enabling them to recombine to form intact NM molecules. This leads to higher threshold collision velocities than found previously in bimolecular collision simulations. The threshold collision velocities determined from the multimolecular and bimolecular collision simulations are higher than the average atomic velocities expected at the detonation shock front, suggesting that molecular dissociation most likely occurs with thermalization after the shock front passes. To probe the pressure induced dissociation mechanism of liquid NM, CPMD simulations were performed under conditions of high pressure compression at low temperatures to avoid strong thermal influence. Compression of liquid NM by factors of 2.0 and 2.5 at 300 K showed no pressure induced molecular dissociation. A proton transfer reaction between two closely spaced NM molecules aligned in an anti-parallel orientation, leading to CH_2NO_2 and $CH_3NO(OH)$, was observed in the CPMD simulation of liquid NM compressed by a factor of 3.0 at 150 K. BP86/DZVP quantum chemical calculations indicate that this reaction is highly endothermic and proceeds with an activation barrier of about 25 kcal/mol.

INTRODUCTION

A detailed understanding of the shock-induced chemical decomposition of molecular liquids at the atomic-level is of particular interest to the fields of energetic materials and detonation science. Nitromethane (NM) is a prototypical energetic molecule that has been the subject of numerous theoretical simulations, due to its small size. A number of classical molecular dynamics (MD) simulations of liquid NM under ambient and shocked conditions have been performed with empirically derived potentials.[1,2] However, simulating the chemical decomposition of molecular liquids is problematic with classical MD, due to the limitations of the parameterized potentials. The tremendous advances in computer hardware coupled with the advent of accurate and efficient quantum chemical methodologies, like density functional theory (DFT), have made computational modeling of energetic materials feasible over the past decade. Recently, it has become possible to perform practical *ab initio* MD simulations of small molecules in both the gas[3] and high pressure condensed phase.[4,5] The Car-Parinnello MD (CPMD)[6] scheme, which usually employs the Kohn-Sham DFT approach in conjunction with a plane-wave pseudopotential basis set, is among the most popular *ab initio* MD approaches.

Although numerous theoretical reports focusing on NM have appeared in the literature the decomposition mechanism of liquid NM under shock conditions remains elusive. The C-N bond is the weakest bond in NM and therefore unimolecular C-N bond scission has often been implicated as the dominant decomposition pathway. However, a number of high pressure studies do not support this mechanism.[7,8] Alternative decomposition mechanisms have been proposed including unimolecular NM rearrangements to form methyl nitrite and nitromethyl aci-anions, as well as several bimolecular mechanisms.[3,9,10] To gain some insight into these decomposition pathways bimolecular collision MD simulations have been performed by a number of researchers.[3,11] Our previous study[11] examined bimolecular collisions of NM in a variety of orientations and a large range of incident collision velocities. In this study, the critical velocity for successful dissociation was found to be 7.0 km/s for the anti-parallel molecular orientation, higher than the average atomic velocities expected at the shock front of the detonation[12]. Although these bimolecular collision simulations provide a qualitative glimpse into the shock-induced dissociation process, they cannot account for the effects that neighboring molecules may have on the dissociation mechanism. This issue is addressed in the first phase of the present contribution, in which we report the results of CPMD simulations of multimolecular collisions of NM.

Metastable, high energy-density materials have been ardently pursued with various technologies, particularly, high-pressure compression. Recently, a non-molecular meta-stable state of nitrogen was found when N_2 was compressed beyond 140 GPa at low temperature.[13] Compression and pressure dissociation of more complex energetic molecular liquids, such as nitromethane, is of great interest in this area. We have examined liquid nitromethane under high pressure conditions with both classical and *ab initio* molecular dynamics simulations, the results of which will be presented in the second phase of this contribution.

COMPUTATIONAL METHODS

All of the *ab initio* MD simulations reported in the present work employed the Car-Parrinello scheme within the Kohn-Sham density functional theory (KS-DFT) framework. The BP86 functional, comprised of Becke's 1988 gradient corrected exchange functional[14] in combination with Perdew's 1986 gradient corrected correlation functional[15], was employed in all of the CPMD simulations. This functional has been shown to predict geometric parameters and dissociation energies for NM in close agreement with values obtained from experiment and high-level correlated MCSCF calculations. To allow for proper dissociation of the NM molecules, the spin unrestricted DFT formalism was employed in all of the simulations. Only the valence electrons were treated explicitly in the simulations, with the valence-core interactions described by the non-local norm-conserving pseudo-potentials of Trouileer and Martins[16] and the valence orbitals expanded in terms of a plane wave basis set with a kinetic energy cutoff of 60 Ry. These parameters provided good energy conservation MD within 3.5×10^{-4} E_h/ps. A fictitious electron mass of 800 a.u. and a time step of 0.145 fs was employed. The CPMD package of Parrinello *et al.*[17] was employed for all of the *ab initio* molecular dynamics simulations reported here.

Multimolecular Collisions: The multimolecular NM collision simulations are qualitatively similar to the bimolecular collisions previously reported.[11] A total of 13 NM molecules were placed in an orthorhombic simulation cell (dimensions $19.0 \times 14.2 \times 14.2$ Å) such that one NM molecule was placed at one end of the simulation cell and the remaining twelve NM molecules were placed at the opposite end of the simulation cell. The simulations were initiated by propelling the separated NM molecule into a stationary NM molecule, embedded in a cluster of 12 NM molecules as illustrated in Figure 1. The cluster of 12 NM molecules are randomly oriented and possess a density of 1.14 g/mL, corresponding to the density of NM at ambient pressure and temperature. The molecular orientations of the two colliding molecules were varied along with the incident collision velocities (6.0 – 12.0 km/s). Each multimolecular collision simulation was run for approximately 0.5 ps or 3500 time steps.
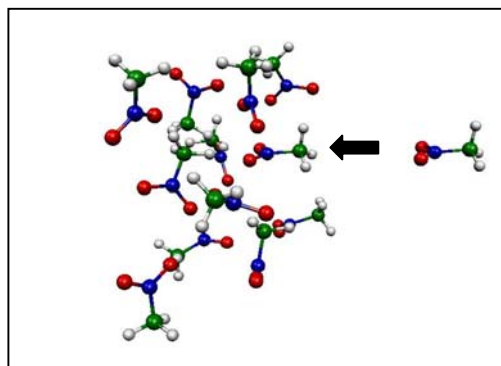

FIGURE 1: MULTIMOLECULAR COLLISION SIMULATION PROCEDURE.

Liquid Simulations: The classical simulations of liquid NM were carried out at 300 K using the potential derived specifically for liquid NM by Politzer *et al.*[1]. The MD trajectories were propagated using either a modified Beeman integration method[18], with maintenance of a desired temperature and/or pressure using the Groningen method of coupling to external baths[19,20]. The Ewald summation technique[21] for inclusion of long range electrostatic interactions via periodic boundaries was used. In all of the classical simulations a time step of 0.5 fs was utilized, and the system was equilibrated for 50 ps followed by a production run for the same duration. The Tinker program of

Ponder and co-workers[22] was employed for all of the classical simulations.

The *ab initio* MD simulations of compressed liquid NM employed a cubic simulation cell containing 32 NM molecules. The length of the simulation cell was determined by compressing the volume of the simulation cell of liquid NM at ambient pressure and temperature by factors of: 2.0, 2.5, and 3.0. The initial geometric configurations of the *ab initio* liquid simulations were obtained from well equilibrated classical simulations. For the compression factor of 3.0, classical simulation resulted in unnatural distortions of the NM molecules and as such the initial geometric configuration was obtained by incrementally compressing the simulation cell from the *ab initio* simulation of liquid NM compressed by a factor of 2.5. The temperature in all of these compressed liquid NM simulations was slowly warmed up from 50 K to 300 K. Initially a short 0.725 ps (5000 time steps) simulation was performed at 50 K, then the temperature was increased to 150 K and another 0.725 ps simulation was performed. The temperature was then raised to 300 K and the system was equilibrated for a total of 3.6 ps (25000 time steps). Following this equilibration stage a production run was performed at 300 K for another 3.6 ps (25000 time steps). Nose-Hoover chain thermostats[20,23] of length 4 at 300 K were employed in all of the equilibration simulations to ensure proper equipartitioning of the energy, however, sampling runs were NVE simulations with thermostats turned off.

RESULTS AND DISCUSSION

Multimolecular Collisions: Schematics of the four collision orientations of the colliding NM molecules in the multimolecular collision simulations investigated are given in Table 1. Also given in Table 1 are the threshold collision velocities (*i.e.*, the lowest collision velocity which leads to permanent bond cleavage) determined for each molecular orientation from the current multimolecular collision simulations, as well as those determined from the previous bimolecular collision simulations.
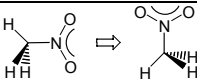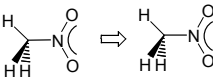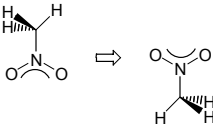
Our previous bimolecular collision simulation results revealed that the C-N bond of the incoming NM molecule is cleaved in nearly all of the orientations investigated.[11] A different decomposition mechanism was observed in only one high velocity collision simulation (the 11.0 km/s velocity bimolecular collision in the offset anti-parallel orientation), in which initial N-O bond cleavage of the stationary NM molecule was observed followed by a series of intermolecular rearrangements leading to the final products: NM, NO and OCH_3. As seen in Table 1, the lowest threshold collision velocity was found to be 7.0 km/s for the offset anti-parallel orientation. The threshold collision velocities for the perpendicular and head-to-tail orientations were found to be slightly higher at 8.0 and 8.5 km/s, while that for the anti-parallel orientation was found to be the highest at 10.5 km/s.

C-N bond cleavage was the predominant mechanism of decomposition in the current multimolecular collision simulations, in agreement with the previous bimolecular collision simulations.[11] A different fragmentation pattern, initial C-H bond scission stationary molecule was observed in one of the high velocity multimolecular collision simulations (12.0 km/s in a head-to-tail orientation). The initial C-H bond cleavage was followed

immediately by the migration of this free H atom to one of the O atoms of the incoming NM molecule which induced N-O bond cleavage of this NM molecule yielding OH and CH_3NO. The N-O bond of the stationary molecule was then cleaved and the free O atom migrated to the CH_2 group of the stationary molecule, thereby inducing C-N bond cleavage to yield CH_2O and NO fragments. The final products produced from this cascade of reactions are: OH, CH_2O, NO, and CH_3NO.

TABLE 1: THRESHOLD COLLISION VELOCITIES DETERMINED FROM MULTIMOLECULAR AND BIMOLECULAR COLLISION SIMULATIONS.

Orientation		Threshold Collision Velocity[a]	
		Multimolecular[b]	Bimolecular[c]
	Perpendicular	12.0	8.0
	Anti-parallel	11.0	10.5
	Head-to-Tail	11.0	8.5
	Offset Anti-parallel	12.0	7.0

[a] Threshold collision velocities given in units of km/s. [b] Values correspond to those determined from our current CPMD multimolecular collision simulations. [c] Values correspond to those determined from our previous CPMD bimolecular collision simulations.

The most serious limitation of the previous bimolecular collision simulations was that they were limited to collision induced reactions involving only the two colliding molecules. The present multimolecular collision simulations offer a substantial improvement since they allow for possible collision induced reactions involving the incoming, stationary, and neighboring NM molecules. Interestingly, we observed collisions involving more than the two colliding NM molecules at only high collision velocities. For example, in the multimolecular collision simulations of the perpendicular molecular orientation at 11.0 and 12.0 km/s we observed collisions between three and four NM molecules, respectively, (the incoming, stationary NM molecules plus one and two neighboring molecules, respectively) resulting in permanent C-N bond cleavage of the stationary molecule, while the other molecules involved recombined to form intact NM molecules.

As evident from Table 1 the threshold collision velocities determined from our multimolecular collision simulations are higher than those found previously from bimolecular collision simulations for each molecular orientation investigated. In all

cases the low velocity multimolecular collisions induce initial C-N bond scission of the incoming and stationary molecules, however, the neighboring NM molecules act as a trap to confine the CH_3 and NO_2 fragments produced, thereby enabling them to recombine to form intact NM molecules. The C-N bond then alternately breaks and reforms as the simulation continues until finally it remains intact when there is insufficient energy to break it. At higher collision velocities the recoiling fragments produced during the initial collision possess enough translational energy to overcome the confinement forces of the neighboring NM molecules leading to permanent cleavage of the C-N bond to yield CH_3 and NO_2. We observed permanent C-N bond scission in both the incoming and stationary NM molecules in the multimolecular collision simulations in the offset anti-parallel orientation (at a collision velocity of 12.0 km/s), while the anti-parallel and head-to-tail orientations (at a collision velocity of 11.0 km/s) displayed permanent C-N bond cleavage of the incoming NM molecule, and the perpendicular orientation (at a collision velocity of 12.0 km/s) displayed permanent C-N bond cleavage of the stationary NM molecule.

Liquid Simulations: *Ab initio* MD simulations are computationally demanding, and we are limited to modeling a small number of molecules over short time scales compared to classical MD simulations. Classical MD simulations of liquid NM with 32, 108, and 256 NM molecules in the simulation cell were performed to investigate the dependence of the observable properties of the liquid on the size of the simulation cell. The densities of liquid NM at various pressures were calculated from classical NPT simulations for these three simulation cells and they are reported in Table 2. The results indicate that at low pressures the densities computed from simulations with 32 NM molecules in the simulation cell are about 6 % smaller than the density calculated from the larger simulation cells containing 108 and 256 NM molecules, and they deviate substantially from the known experimental value of 1.139 g/cm^3 at 1 atm. As the pressure increases the agreement between the density computed from the simulation employing 32 molecules in the simulation cell and that computed from the simulations employing the larger simulation cells becomes significantly better and the results appear to be converging with respect to the size of the simulation cell. At the highest pressure investigated, the deviation between the density computed from the simulation employing a 32 molecule simulation cell and that computed from the simulation cell employing the 256 molecule simulation cell was less than 1 %. Based on these classical MD simulations a small 32 molecule simulation cell reproduces the results obtained with larger simulation cells for liquid NM under mid to high pressure regimes and it should adequately model bulk liquid NM in our CPMD simulations.

We carried out classical and *ab initio* Car-Parinello MD simulations of liquid NM at 1 atm and 1.0×10^5 atm in an effort to understand how the first principles potential differs from the empirical potential. To address this issue, we compared the O-O and O-H pair correlation functions derived from classical and *ab initio* MD simulations of liquid NM at pressures of 1 and 1.0×10^5 atm (see Figure 2). The plots in Figure 2 show that overall there is a good agreement between the classical and *ab initio* simulations at both the low and moderate pressure regimes. A closer examination of the pair correlation functions reveals that the DFT potential is softer than the classical potential, enabling

the NM molecules to approach closer to one another than in the classical simulations.

TABLE 2: CALCULATED DENSITIES OF LIQUID NITROMETHANE WITH VARYING SIMULATION CELL SIZE AT DIFFERENT PRESSURES.[a,b,c]

Pressure	Calculated Liquid Bulk Density		
	32 Molecule Cell	108 Molecule Cell	256 Molecule Cell
1.0	1.031 ± 0.012	1.101 ± 0.006	1.147 ± 0.002
1.0×10^4	1.312 ± 0.006	1.343 ± 0.004	1.349 ± 0.003
5.0×10^4	1.606 ± 0.003	1.615 ± 0.002	1.613 ± 0.001
1.0×10^5	1.752 ± 0.002	1.764 ± 0.001	1.764 ± 0.001
1.4×10^5	1.833 ± 0.002	1.846 ± 0.001	1.845 ± 0.001

[a] Densities correspond to those obtained from classical NPT simulations.
[b] Thermodynamic averages were collected for a duration of 0.1 ps and 500 independent data points were employed in the statistical analyses. [c] Densities and pressures are given in units of g/cm³ and atm, respectively.
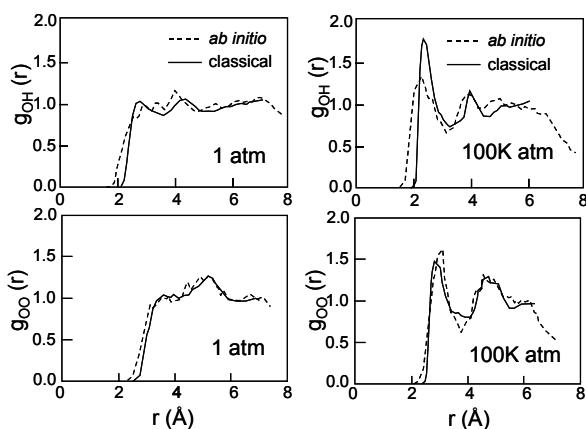

FIGURE 2: O-H AND O-O PAIR CORRELATION FUNCTIONS DERIVED FROM CLASSICAL AND *AB INITIO* MD SIMULATIONS OF LIQUID NM AT 1 and 1.0×10^5 ATM.

The current CPMD simulations of compressed liquid NM show no molecular decomposition at compression factors of 2.0 and 2.5 at 300 K. However, when the liquid is compressed by a factor of 3.0 an interesting pressure induced molecular decomposition is observed at 150 K after equilibration for about 3300 time steps. An intermolecular H atom transfer event occurs between two very closely spaced molecules aligned in an anti-parallel alignment, as illustrated in the MD trajectory snapshots shown in Figure 3. As illustrated in Figure 3, the CH_3 group of one of the NM molecule re-orients itself such that two of its H atoms lie in the same plane as the NO_2 fragment and the other H atom is oriented nearly perpendicular to this plane directed at the O atom of the adjacent NM molecule. This H atom then transfers from the C atom of the first NM molecule to the O atom of the second NM molecule to yield the final products CH_2NO_2 and $CH_3NO(OH)$. The H transfer event occurs on a time scale of about 15 fs.

The coordinates of the two NM molecules involved in this H transfer event were extracted from the CPMD trajectory and a preliminary reaction pathway was constructed from BP86/DZVP single point energy calculations at their respective

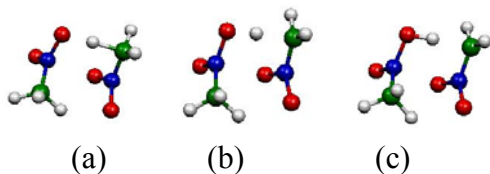geometric orientations. (These single point energy calculations employed the ADF quantum chemistry program suite.[24])

(a) (b) (c)

FIGURE 3: SNAPSHOTS OF THE PROTON TRANSFER REACTION OBSERVED IN THE CPMD SIMULATION OF LIQUID NM COMPRESSED BY A FACTOR OF 3.0.

Based on the changes in atomic charges and bond lengths this reaction can be classified as a proton transfer reaction as illustrated in Figure 4. Our calculations predict this proton transfer reaction to be highly endothermic (estimated to be 50 kcal/mol from gas phase calculations of the two molecules in the "supermolecule"

geometry extracted from the MD trajectory of the compressed liquid and 190 kcal/mol for the reaction in the gas phase). The activation barrier is predicted to be about 25 kcal/mol based on our calculated proton transfer reaction pathway. Given that this proton transfer reaction is predicted to be highly unfavorable and the temperature of the simulation at which we observed this event was 150 K, we postulate that this reaction is driven by the reduction in volume of the final products under these high pressure conditions.

The planar CH_2NO_2 molecule produced will occupy a smaller volume than the original NM molecule. Therefore, the resultant products will occupy less volume than the two original NM molecules, thereby leading to a more favorable geometric orientation in the highly compressed liquid. We are currently examining if this proton transfer is a rare event or a common dissociation mechanism at high compression factors.
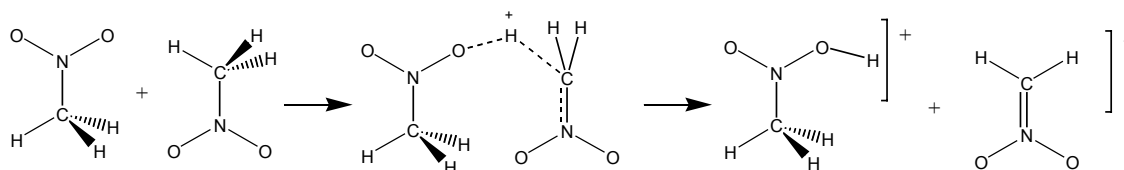

FIGURE 4: SCHEMATIC OF THE PROTON TRANSFER REACTION OBSERVED IN THE HIGHLY COMPRESSED LIQUID NM CPMD SIMULATION.

SUMMARY AND CONCLUSIONS

The mechanism of shock induced chemical decomposition of nitromethane was investigated through *ab initio* MD simulations of multimolecular collisions. Although our rationale for extending the bimolecular collision simulations to

multimolecular collision simulations was to account for potential collision induced reactions involving multiple NM molecules, the current CPMD simulations indicate that this only occurs at very high incident collision velocities. In accord with previous bimolecular collision simulations C-N bond cleavage is the primary

mechanism of NM dissociation in the multimolecular collision simulations. An alternative C-H bond scission fragmentation pattern was observed in only one of the high collision velocity simulations leading to OH, CH_2O, NO, and CH_3NO final products. The threshold collision velocities determined from the multimolecular collision simulations were higher than the values determined previously from bimolecular collision simulations. The neighboring NM molecules confine the CH_3 and NO_2 fragments produced from the initial C-N dissociation of the incoming and stationary NM molecules, thereby enabling them to recombine to reform intact NM molecules. High collision velocities are necessary to overcome this confinement and permanently break the C-N bond. The threshold collision velocities determined from both the multimolecular and bimolecular collision simulations are higher than the average atomic velocities expected at the detonation shock front indicating that molecular dissociation most likely occurs with thermalization after the initial shock front passes. In the future we will expand this work to investigate more complex collision scenarios, such as the collision between a wall of NM molecules and a cube of nitromethane molecules, as a model of the shock front propagation through the bulk liquid.

Comparison of the classical MD simulations with 32, 108, and 256 NM molecules in the simulation cell indicates that the results obtained with the smallest simulation cell are in good agreement with those obtained with larger simulation cells for moderate pressures where the empirical potential employed is valid. The pair correlation functions obtained from the *ab initio* and classical MD simulations show good agreement at 1 and 1.0×10^5 atm, although the DFT potential is softer than the classical potential. *Ab initio* MD simulations of high pressure compression under conditions of low temperature were employed to investigate pressure-induced molecular dissociation under minimal thermal influence. These simulations show no molecular dissociation of NM up to a compression factor of 2.5 at 300 K, while the simulation at a compression factor of 3.0 at 150 K indicates the possibility of an intermolecular proton transfer event. Static DFT calculations predict this proton transfer event to be highly endothermic (50 – 190 kcal/mol) and to have an activation barrier of about 25 kcal/mol. We postulate that it is the reduced volume of the planar CH_2NO_2 molecule produced which drives this initial molecular decomposition reaction under these high pressure conditions. In the future, we would like to establish if this proton transfer reaction is a common mechanism of molecular decomposition in liquid NM under high pressure as well as determine alternative decomposition mechanisms that may be prominent in highly compressed liquids.

REFERENCES

1. Alper, H.E., Abu-Awwad, F. and Politzer, P. J. Phys. Chem. B, Vol. 103, 1999, pp. 9738.
2. Sorescu, D.C., Rice, B.M. and Thompson, D.L. J. Phys. Chem. A, Vol. 105, 2001, pp. 9336.
3. Haskins, P.J. and Cook, M.D. Shock Compression of Condensed Matter, Schmidt, Dandekar and Forbes (Eds.), 1997, p. 305.
4. Kress, J.D., Mazevet, S. and Collins, L.A. Phys. Rev. B, Vol. 63, 2000, pp. 024203/1.
5. Reed, E.J., Joannopoulos, J.D. and Fried, L.E. Phys. Rev. B, Vol. 62, 2000, pp. 16500.

6. Car, R. and Parrinello, M. Phys. Rev. Lett., Vol. 55, 1985, pp. 2471.
7. Winey, J.M. and Gupta, Y.M. J. Phys. Chem. B, Vol. 101, 1997, pp. 10733.
8. Piermarini, G.J., Block, S. and Miller, P.J. J. Phys. Chem., Vol. 93, 1989, pp. 457.
9. Bardo, R.D. Int. J. Quantum Chem. Symp., Vol. 20, 1986, pp. 455.
10. Bardo, R.D., Ninth Symposium (International) on Detonation, Office of Naval Research, Arlington, VA, 1989, p. 235.
11. Wei, D., Zhang, F. and Woo, T.K., Proceedings of the 12th Biennial International Conference of the APS Topical Group on Shock Compression of Condensed Matter, Atlanta, GA, 2001.
12. Graham, R.A. J. Phys. Chem., Vol. 83, 1979, pp. 3048.
13. Eremets, M.I., Hemley, R.J., Mao, H.K. and Gregoryanz, E. Nature, Vol. 411, 2001, pp. 170.
14. Becke, A. Phys. Rev. A, Vol. 38, 1988, pp. 3098.
15. Perdew, J.P. Phys. Rev. B, Vol. 33, 1986, pp. 8822.
16. Trouiller, N. and Martins, J.L. Phys. Rev. B, Vol. 43, 1991, pp. 1993.
17. Hutter, J., Alavi, A., Deutsch, T., Bernasconi, M., Goedecker, S., Marx, D., Tuckerman, M. and Parrinello, M., CPMD. MPI fur Festkorperforschung and IBM Zurich Research Laboratories, 1995-1999.
18. Beeman, J. J. Comput. Phys., Vol. 20, 1976, pp. 130.
19. Berendsen, H.J.C., Postma, J.P.M., van Gunsteren, W.F., DiNola, A. and Haak, J.R. J. Chem. Phys., Vol. 81, 1984, pp. 3684.
20. Hoover, G. Phys. Rev. A, Vol. 31, 1985, pp. 1695.
21. Toukmaji, A.K. and Board, J.A.J. Comp. Phys. Commun., Vol. 95, 1996, pp. 73.
22. Ponder, J.W., Tinker. Washington University, St. Louis, MO, 1997.
23. Nose, S. J. Chem. Phys., Vol. 81, 1984, pp. 511.
24. ADF2002.01. SCM, Theoretical Chemistry, Vrije Universiteit, Amsterdam, The Netherlands, 2002.